

UC Davis

UC Davis Previously Published Works

Title

Chemical Characterization and Source Apportionment of Atmospheric Particles Across Multiple Sampling Locations in Faisalabad, Pakistan

Permalink

<https://escholarship.org/uc/item/8289p922>

Journal

CLEAN - Soil Air Water, 44(7)

ISSN

0323-4320

Authors

Javed, Wasim
Wexler, Anthony S
Murtaza, Ghulam
et al.

Publication Date

2016-07-01

DOI

10.1002/clen.201500225

Peer reviewed

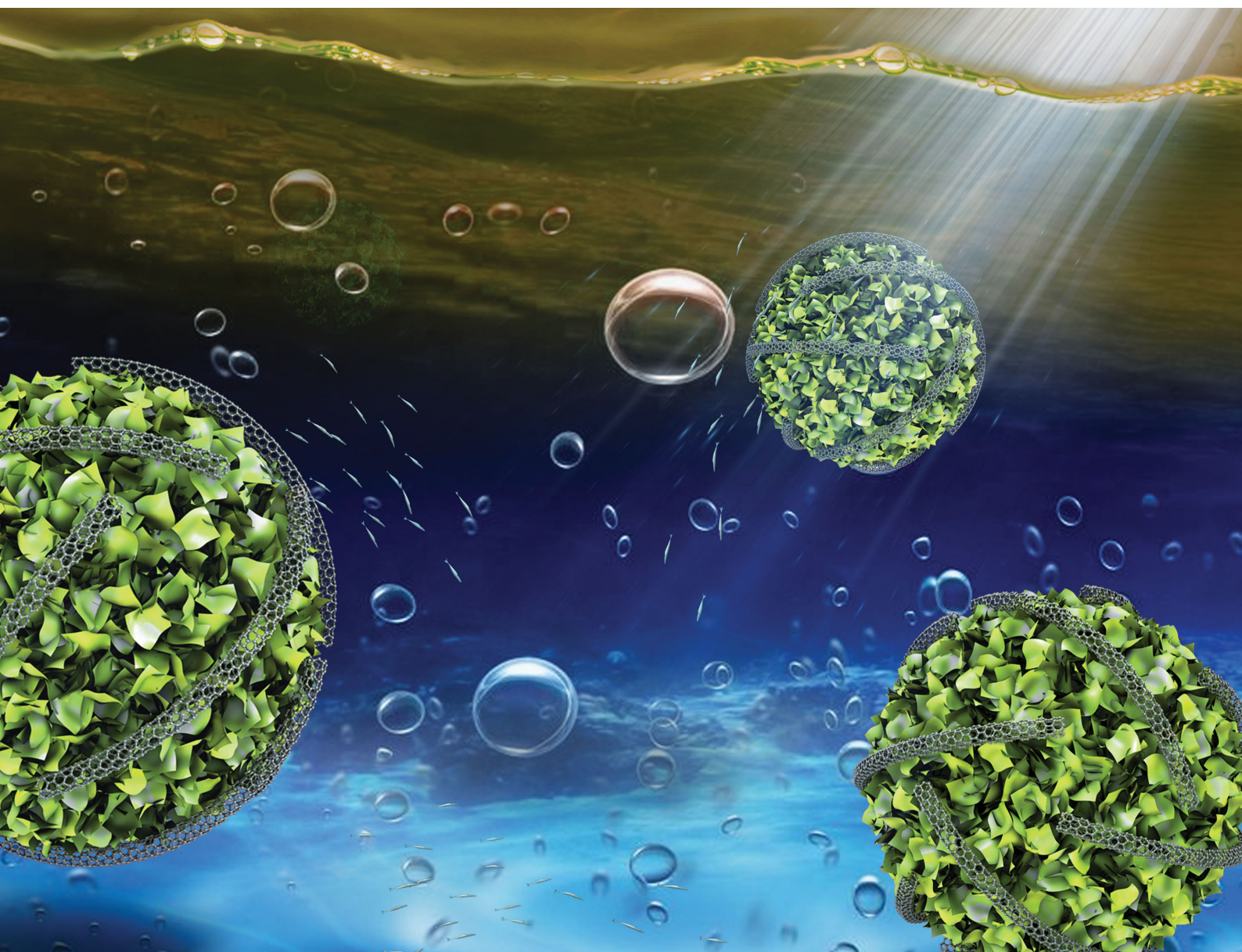
CLEAN

Soil Air Water

Renewables

Sustainability

Environmental Monitoring



Wasim Javed^{1,2}
Anthony S. Wexler³
Ghulam Murtaza¹
Muhammad Mazhar Iqbal¹
Yongjing Zhao³
Tayyaba Naz¹

¹Institute of Soil & Environmental Sciences, University of Agriculture, Faisalabad, Pakistan

²Mechanical Engineering Program, University of Texas A&M at Qatar, Doha, Qatar

³Air Quality Research Center, University of California-Davis, Davis, CA, USA

Research Article


Chemical Characterization and Source Apportionment of Atmospheric Particles Across Multiple Sampling Locations in Faisalabad, Pakistan

Atmospheric particles (total suspended particles, TSPs) mass samples (288) were collected by high volume samplers at nine sampling locations in Faisalabad, Pakistan from May 2012 to April 2013. These TSP mass samples were subjected to gravimetric and quantitative chemical analyses for determining trace elements (Pb, Cd, Ni, Zn, Cu, Fe) using atomic absorption spectroscopy and water-soluble cations (Ca^{2+} , Mg^{2+} , Na^+ and K^+ , NH_4^+) and anions (Cl^- , SO_4^{2-} , and NO_3^-) by ion chromatography. The average TSP mass and elemental concentrations at all locations were found to be highest during the dry and lowest during the wet season. The crustal elements Ca, Fe, Mg, and Na were the largest contributors to TSP mass while elements of anthropogenic origin Pb, Cd, Ni, Cu, and Zn had relatively lower concentrations and also showing a high spatial variation. The concentration of TSP and elements exhibited the maxima at the sampling locations characterized by intensive industrial and vehicular activities. The wind rose analysis and the UNMIX model applied to chemical speciation data both identified the same three primary sources of TSP: power plant/refinery, brick kilns, and roadways. The normalized dot product was successfully used to quantify the similarity between different source profiles extracted from UNMIX model. The coupling of UNMIX with wind direction analysis complemented each other and provided a complete assessment of source contributions and locations.

Keywords: Elements; Source identification; Total suspended particles; UNMIX; Wind roses

Received: April 8, 2015; *revised:* October 17, 2015; *accepted:* February 22, 2016

DOI: 10.1002/clean.201500225

 Additional supporting information may be found in the online version of this article at the publisher's web-site.

1 Introduction

Over the last two decades, air pollution has become a serious environmental concern in developing countries like Pakistan, as a consequence of rapid urbanization and industrialization coupled with increased transportation and energy demands. In particular, urban centers are facing the menace of air pollution primarily due to the presence of particulate matter (PM) and its associated trace metals in the atmosphere [1, 2]. Numerous epidemiological investigations have demonstrated a strong association between ambient PM

concentrations and respiratory- and cardiovascular-related increases in morbidity and mortality especially in urban areas [3].

Characterizing the chemical composition of atmospheric PM and identifying its primary sources are necessary steps for successfully instituting mitigation measures and effective regulatory policies that minimize consequent health impacts [4, 5]. Some periodic reports revealed that atmospheric PM and its associated trace metals have severe environmental and health concerns in the urban areas of Pakistan [1, 2, 4–7]. Meteorology affects transport and transformation of PM in the atmosphere, some source strengths, and can be useful for a better characterization of PM and source identification [9–12].

Source apportionment/identification by receptor modeling has always been a useful tool for establishing emissions regulations. Over the past two decades, models such as chemical mass balance (CMB), principal component analysis (PCA), and positive matrix factorization (PMF), have been used in this regard by many researchers [1, 2, 4–6, 10, 13–15]. During past few years, the UNMIX model has been effectively used as a valuable tool to produce satisfactory results regarding source apportionment comparable

Correspondence: Dr. Wasim Javed, Mechanical Engineering Program, University of Texas A&M at Qatar, Qatar Foundation, Doha 23874, Qatar
E-mail: wasim.javed@qatar.tamu.edu

Abbreviations: AAS, atomic absorption spectrophotometry; CMB, chemical mass balance; PCA, principal component analysis; PM, particulate matter; PMF, positive matrix factorization; SL, sampling location; TSP, total suspended particles; US EPA, United States Environmental Protection Agency; WHO, World Health Organization.

Nine different sampling locations were selected to represent different urban, industrial, and rural settings located downwind, to the North and East, of the city center as shown in Fig. 1. Supporting Information Tab. S1 presents sampling location details. The selection of multiple sampling locations was made based on the existing anthropogenic activities responsible for air pollution, prevailing wind direction for pollutants distribution and dispersion, and to identify sources and their relative contribution to ambient air quality.

2.2 Monitoring and sampling procedure

TSP mass concentrations were monitored with a MicroDust Pro Real-Time Aerosol Monitor (model HB3275-07, Casella CEL, UK) on a 6 h average basis at each sampling location. The instrument has a detection range of $0.001\text{--}2500\text{ mg m}^{-3}$ with a resolution of 0.001 mg m^{-3} . TSP samples were collected on micro-glass-fiber filter papers (47 mm) using a high volume air sampler (model CF-1001BRL, Hi-Q, USA). The sampler flow rate was 85 L m^{-1} with manual compensation for the increased pressure drop across the filter as it loads. The samplers were deployed at 100 m distance and upwind side of the adjacent roads. There were no trees, buildings, and any obvious PM sources within 100 m around the sampling site.

The sampling was done during 2 months of each season, *i.e.*, in May and June 2012, for the summer period, August and September 2012, for the monsoon, December 2012, and January 2013, for winter and March and April 2013, for spring. On sampling day, two 6-h samples were collected during daytime from 7 am to 1 pm and then 1–7 pm. In total, 288 TSP samples were collected at nine sampling locations during the four sampling periods. Each sampling period has four sampling days or eight 6-h samples at each sampling location. In addition, 36 (four per site) field blanks were also collected. The TSP mass was also determined gravimetrically from the filters after conditioning in a desiccator for 24 h at $45 \pm 5\%$ relative humidity and $23 \pm 3^\circ\text{C}$. The method detection limit for TSP mass was $5\text{ }\mu\text{g m}^{-3}$. The filter papers containing PM were placed in sealed plastic Petri dishes and stored at -20°C before analysis.

2.3 Analytical assay

After gravimetric analysis, each filter was cut into two equal parts. One-half was used for the determination of trace metals after digestion in nitric acid (Suprapure, 65% GR grade, Merck) and perchloric acid (Suprapure, 70% GR grade, Merck), 10:1, v/v, facilitated by heating [16]. The extracted solution was filtered and diluted to 100 mL with double distilled water and kept in the refrigerator in cleaned polyethylene bottle until analysis. The same procedure was carried out for filter and reagent blanks. Selected trace metals were determined by atomic absorption spectrophotometry (AAS) (Thermo AA, Solar-Series) following Method IO-3.2 [17]. The estimated detection limits (three times the standard deviation of nine blanks analyzed) were 0.005, 0.1, 0.01, 0.02, 0.02, and $0.05\text{ }\mu\text{g mL}^{-1}$ for Cd, Pb, Ni, Zn, Cu, and Fe, respectively.

The other half of the filter was used for determination of water-soluble elemental cations (Ca^{2+} , Mg^{2+} , Na^+ and K^+ , NH_4^+) and anions (Cl^- , SO_4^{2-} , and NO_3^-) after extraction in distilled-deionized water (having a resistivity of $18\text{ M}\Omega\text{ cm}$) by ultrasonication for 2 h [14]. Ionic species were analyzed by ion chromatography (IC

Vario-940 Metrohom, Switzerland). The estimated detection limits were 0.03, 0.02, 0.02, 0.03, 0.05, 0.05, 0.05, and $0.03\text{ }\mu\text{g mL}^{-1}$ for Na^+ , Ca^{2+} , Mg^{2+} , K^+ , NH_4^+ , Cl^- , NO_3^- , and SO_4^{2-} , respectively. The peak areas were calibrated by analyzing a series of standards over the range $0.02\text{--}10\text{ mg L}^{-1}$. The recovery of the elements and ions was in the range of 80–110%, and the precision based on duplicate spiked samples was $\pm 5\%$.

2.4 Quality assurance

An intensive quality assurance program was implemented to maintain the accuracy and precision throughout the study. The United States Environmental Protection Agency (US EPA) procedures/guidelines for ambient air quality monitoring were followed for sampling and laboratory analysis. The flow rates of the aerosol monitor and high volume air sampler were calibrated daily before sampling. For TSP gravimetric and chemical analysis, field blanks, filter paper, and reagent blanks were also used to minimize the error. Filter and reagent blank concentrations were always $<10\%$ of the loaded filter values. To estimate the uncertainty associated with the TSP gravimetric and chemical analysis, 5% duplicate samples were also collected. The results of the duplicate analysis showed $\pm 5\%$ variation in TSP mass and $\pm 10\%$ variation in elemental concentrations that indicates the reliability of the data generated.

Laboratory testing conducted in a manner to ensure the precision and accuracy at all stages. All chemicals and solvents used were of analytical reagent grade procured from Merck (Darmstadt, Germany). The atomic absorption spectrophotometer was standardized with a series of standard solutions supplied by the manufacturer (Thermo Electron S series; Thermo Scientific, Waltham, Mass). The reproducibility test that indicates the stability of the instruments exhibited the relative standard deviation from 97 to 101% with the average relative deviation $<5\%$. Inter-laboratory comparison of the AAS results was also performed at an independent laboratory (Hi-tech Laboratory, University of Agriculture-Faisalabad) and normally, a maximum of $\pm 10\%$ deviation was recorded in the results of the two laboratories.

2.5 Source identification

2.5.1 Wind direction analysis

Wind speed and direction were also determined with a Portable Weather Station (model 110-WS-18, Nova Lynx, USA) with a temporal resolution of 5 min at each sampling location. Then 6 h average wind direction was computed by treating all angular measurements as points on the unit circle and computing the resultant vector of the unit vectors determined by data points [18].

Pollutant roses are indispensable tools to identify unknown sources of particulate heavy metals. Pollutant wind roses were drawn by coupling average (6 h) pollutant concentrations and wind direction data at each sampling location [8, 10–12]. Each wind rose has 16 wind sectors ($0\text{--}360^\circ$), where each petal represents the average concentration of the element in the sector that the wind is blowing from during the sampling period. The indicated wind direction suggests the direction of the source from the sampling location, considering that the source is not too distant from the sampling sites as reported by Javed et al. [19].

2.5.2 Application of UNMIX model

A receptor model “EPA UNMIX v6.0” was used for PM source identification. The EPA UNMIX 6.0 Fundamentals User Guide [20] was followed to optimize the model run conditions. Recently, it has been used in several similar studies [13–15, 21]. UNMIX was used along with wind roses to identify elemental signatures for each major source category as previously indicated by wind direction analysis. The combination of wind direction analysis and UNMIX results indicate more specifically source contributions to each monitoring location.

Firstly, the model was run separately on the elemental concentrations associated with the directions of the three possible sources identified by the wind rose analysis (*i.e.*, power plant/refinery, brick kilns, and roadways). The whole sample composition dataset was filtered into three groups having the element concentration values only from the direction of that particular source at each location. Each group had 68, 64, and 78 samples for power plant/refinery, brick kilns, and roadways oriented UNMIX runs, respectively. Then, UNMIX was also applied to the sample dataset for the dry ($n = 216$) and wet ($n = 72$) seasons, separately.

For the UNMIX runs, TSP mass was excluded as not indicative of a particular source. Also secondary ions (NH_4^+ , Cl^- , SO_4^{2-} , and NO_3^-) were excluded due to their non-specific, long-distance, and secondary sources, as having the emphasis only on identification of local sources in the study area as indicated by Javed et al. [19]. Moreover, since K has a higher variation of about 88% by the model due to spatially dispersed emission sources (biomass burning in the household, brick kilns, agriculture burnings, and textile boilers), it was excluded from the final analysis. We followed strict UNMIX criteria to determine sources (*i.e.*, explained variance is always $>80\%$, and the signal-to-noise ratio >2) in a feasible solution [20]. The concentration time series plots and influential plots were then examined to find out any influential point and to exclude these from the data. In all cases, the feasible model run gave Min signal-to-noise ratio >2 and Min r^2 value $>80\%$ which showed that the results are robust. Also, high R^2 values of the measured and UNMIX predicted concentrations of selected elements showed that the model performed well (*e.g.*, Supporting Information Tab. S2). Supporting Information Figs. S1–S3 show some feasible solution conditions of UNMIX run for the dry season.

2.5.3 Normalized dot product

One way to quantify the similarity between different source profiles extracted from the model is to take the normalized dot product of the corresponding components of two vectors (*e.g.*, source profiles) [22, 23]. If the normalized dot product is 1, the source profiles are identical. The degree to which they are below 1 indicates their dissimilarity. Each feature component (x_1, x_2, \dots, x_N) is normalized independently to distribute the feature values in the [0,1] range by using Eq. (1):

$$x'_i = \frac{x_i}{\sqrt{\sum_{i=1}^N x_i^2}} \quad (1)$$

The dot product of two vectors x and y can be calculated as [23]:

$$x \cdot y = \sum_{i=1}^N x'_i y'_i \quad (2)$$

where x'_i and y'_i are the normalized components or coordinates of x and y vectors.

3 Results and discussion

3.1 TSP mass and element concentrations

A maximum of $\pm 10\%$ deviation was observed between the two methods for determining TSP mass while the real-time monitor over-measured TSP mass concentration as compared to the high volume sampler (Supporting Information Fig. S4). The average mass concentrations of TSP and elemental species ($n = 288$) at selected sampling locations during the dry and wet sampling periods (May 2012–April 2013) are summarized in Tab. 1. Samples were classified as dry (summer, winter, and spring; $n = 216$) and wet (monsoon; $n = 72$) depending on the occurrence of rainfall during the sampling periods. The differences in TSP mass and elemental concentrations at all locations were statistically significant ($p < 0.001$) with higher levels during the dry season as expected. The lower levels observed during the wet season can be attributed to the wash-out effect of rainfall, wet surfaces, and higher relative humidity that reduces the resuspension of the road and crustal dust [4, 5, 14, 24] and also shutdown of brick kilns during the wet (rainy) season. Higher concentrations were found during the dry period likely due to the enhanced resuspension of the road and crustal dust favored by higher temperature and wind speed, coupled with lower rainfall and relative humidity [1, 2, 9, 15]. Also, brick kilns operate during the dry season while the most do not operate during the wet season.

The average TSP concentrations at all locations were $645 \mu\text{g m}^{-3}$ with a range of $115\text{--}1422 \mu\text{g m}^{-3}$ during the dry season and $365 \mu\text{g m}^{-3}$ with a range of $86\text{--}658 \mu\text{g m}^{-3}$ during the wet season (Tab. 1). The highest TSP concentration was observed at SL2 (1422 and $658 \mu\text{g m}^{-3}$) followed by SL3 with concentrations of 1186 and $588 \mu\text{g m}^{-3}$ during dry and wet periods, respectively. These locations are characterized by intensive industrial activities with heavy on road traffic. Similar higher TSP concentrations were observed at SL1, SL4, and SL6 sampling locations, which is in agreement with similar human activities at these dense commercial urban areas. The more remote rural location, SL9, had the lowest TSP concentration of 115 and $86 \mu\text{g m}^{-3}$ during dry and wet periods, respectively. TSP concentrations at all locations except SL9 were much higher than the 24-h limit values of 120 and $260 \mu\text{g m}^{-3}$ recommended by the World Health Organization (WHO) [25] and US EPA [26], respectively.

Elemental concentrations followed the same seasonal pattern as TSP concentrations – higher in the dry season, lower in the wet season. The crustal elements Ca, Fe, Na were the largest contributors to TSP and showing a significant location-to-location variation [15, 27, 28]. Elements of anthropogenic origin, *i.e.*, Pb, Cd, Ni, Cu, Zn had relatively lower concentrations. In Pakistan, Pb is still being used as an anti-knocking agent in gasoline regardless of a ban on the leaded fuel, because compliance is not enforced yet [4]. Also, Pb has become a part of the road dust due to the use of leaded fuel over the years [14, 29]. The likely Ni source was crude oil combustion in a power plant and oil refinery located near and upwind of the sampling sites [19, 21]. While Zn and Cu are mostly emitted from lubricant oil, brake linings, and tire wear of poorly maintained and old vehicles plying on the roads [2, 4]. Use of low-quality coal, wood, used rubber tires, and waste oil as a fuel in brick

Table 1. Ambient TSP and elemental concentrations \pm SD ($\mu\text{g m}^{-3}$) in TSP ($n = 288$) at different sampling locations during dry and wet seasons

	Sampling location										Mean
	SL1	SL2	SL3	SL4	SL5	SL6	SL7	SL8	SL9	SL10	
TSP	830 \pm 200 ^{b)}	1422 \pm 320	1186 \pm 270	691 \pm 180	363 \pm 110	504 \pm 140	296 \pm 90	404 \pm 120	115 \pm 25	645 \pm 160	
	525 \pm 160	658 \pm 210	588 \pm 190	325 \pm 70	290 \pm 90	322 \pm 90	205 \pm 60	286 \pm 80	86 \pm 20	365 \pm 110	
Pb	3.9 \pm 0.3	4.2 \pm 0.4	4.0 \pm 0.4	3.8 \pm 0.3	3.1 \pm 0.3	3.6 \pm 0.3	2.8 \pm 0.2	3.4 \pm 0.3	1.1 \pm 0.1	3.3 \pm 0.3	
	2.0 \pm 0.2	2.4 \pm 0.4	2.1 \pm 0.2	1.9 \pm 0.2	1.5 \pm 0.1	1.8 \pm 0.1	1.3 \pm 0.1	1.5 \pm 0.1	0.8 \pm 0.1	1.7 \pm 0.2	
Cd	0.037 \pm 0.005	0.041 \pm 0.006	0.039 \pm 0.005	0.034 \pm 0.005	0.026 \pm 0.005	0.029 \pm 0.006	0.022 \pm 0.004	0.024 \pm 0.006	0.011 \pm 0.002	0.029 \pm 0.005	
	0.017 \pm 0.004	0.019 \pm 0.005	0.018 \pm 0.003	0.014 \pm 0.004	0.012 \pm 0.004	0.012 \pm 0.004	0.010 \pm 0.003	0.012 \pm 0.003	0.005 \pm 0.002	0.013 \pm 0.004	
Ni	1.5 \pm 0.3	1.6 \pm 0.4	1.5 \pm 0.3	1.5 \pm 0.3	1.0 \pm 0.2	1.4 \pm 0.4	1.1 \pm 0.3	0.77 \pm 0.21	0.49 \pm 0.11	1.2 \pm 0.3	
	0.84 \pm 0.23	0.91 \pm 0.17	0.76 \pm 0.24	0.70 \pm 0.21	0.48 \pm 0.15	0.69 \pm 0.19	0.57 \pm 0.2	0.35 \pm 0.11	0.30 \pm 0.08	0.62 \pm 0.17	
Zn	11.8 \pm 2.3	10.4 \pm 2.4	11.4 \pm 2.8	9.8 \pm 2.5	8.4 \pm 2.2	11.1 \pm 2.1	6.8 \pm 1.8	9.5 \pm 2.4	3.2 \pm 0.6	9.1 \pm 2.1	
	7.1 \pm 1.9	6.4 \pm 2.1	8.0 \pm 2.3	5.5 \pm 1.3	4.2 \pm 1.4	6.6 \pm 1.1	3.6 \pm 1.0	4.3 \pm 1.3	1.8 \pm 0.4	5.3 \pm 1.4	
Fe	13.6 \pm 2.3	11.6 \pm 2.5	12.3 \pm 2.2	9.9 \pm 2.2	7.7 \pm 1.6	13.2 \pm 3.1	8.5 \pm 2.1	9.4 \pm 1.9	3.6 \pm 0.6	9.9 \pm 2.1	
	8.5 \pm 1.9	8.2 \pm 2.4	7.2 \pm 1.5	6.7 \pm 2.5	3.6 \pm 0.9	7.7 \pm 2.0	4.3 \pm 1.4	5.56 \pm 1.9	2.0 \pm 0.4	6.0 \pm 1.7	
Cu	7.3 \pm 1.2	8.3 \pm 1.1	7.4 \pm 1.2	6.8 \pm 1.2	4.3 \pm 0.9	6.3 \pm 1.0	5.2 \pm 0.9	5.7 \pm 0.9	1.8 \pm 0.3	5.9 \pm 0.9	
	3.6 \pm 0.7	3.4 \pm 0.6	3.1 \pm 0.8	2.9 \pm 0.8	1.3 \pm 0.3	2.5 \pm 0.7	1.8 \pm 0.3	2.1 \pm 0.5	0.96 \pm 0.21	2.4 \pm 0.6	
Mg ²⁺	6.0 \pm 0.9	6.7 \pm 0.9	5.9 \pm 1.0	5.6 \pm 0.9	3.5 \pm 0.8	5.1 \pm 0.8	4.2 \pm 0.7	4.6 \pm 0.8	1.4 \pm 0.3	4.8 \pm 0.8	
	2.9 \pm 0.6	2.8 \pm 0.5	2.5 \pm 0.6	2.4 \pm 0.7	1.1 \pm 0.3	2.1 \pm 0.6	1.5 \pm 0.3	1.7 \pm 0.4	0.8 \pm 0.2	1.9 \pm 0.4	
Na ⁺	10.3 \pm 2.1	9.1 \pm 2.2	9.9 \pm 2.5	8.6 \pm 2.2	7.4 \pm 1.9	9.7 \pm 1.8	5.9 \pm 1.5	8.3 \pm 2.1	2.8 \pm 0.5	8.0 \pm 1.8	
	6.2 \pm 1.7	5.6 \pm 1.9	7.0 \pm 2.0	4.8 \pm 1.1	3.6 \pm 1.2	5.8 \pm 0.9	3.1 \pm 0.8	3.8 \pm 1.1	1.5 \pm 0.3	4.6 \pm 1.2	
Ca ²⁺	14.9 \pm 2.6	12.6 \pm 3.1	13.5 \pm 1.5	10.9 \pm 2.4	8.5 \pm 1.8	14.5 \pm 3.4	9.3 \pm 2.3	10.3 \pm 2.2	3.9 \pm 0.7	10.9 \pm 2.2	
	9.4 \pm 2.1	9.6 \pm 2.2	7.6 \pm 1.1	7.4 \pm 2.7	4.0 \pm 1.1	8.5 \pm 2.2	4.8 \pm 1.6	6.2 \pm 2.1	2.3 \pm 0.4	6.6 \pm 1.7	
K ⁺	12.9 \pm 2.6	11.5 \pm 2.7	12.5 \pm 3.1	10.8 \pm 2.7	9.3 \pm 2.3	12.2 \pm 2.3	7.4 \pm 1.9	10.5 \pm 2.7	3.6 \pm 0.7	10.1 \pm 2.4	
	7.8 \pm 2.1	7.1 \pm 2.3	8.8 \pm 2.4	6.1 \pm 1.4	4.6 \pm 1.5	7.3 \pm 1.2	3.9 \pm 1.1	4.8 \pm 1.4	1.9 \pm 0.4	5.8 \pm 1.6	
NH ₄ ⁺	20.7 \pm 5.1	19.5 \pm 4.7	18.7 \pm 5.3	17.5 \pm 3.6	14.5 \pm 3.1	18.1 \pm 3.6	14.6 \pm 2.8	10.4 \pm 2.5	7.4 \pm 1.9	15.7 \pm 3.6	
	9.4 \pm 3.0	8.8 \pm 3.3	7.6 \pm 2.5	8.9 \pm 3.7	6.8 \pm 2.0	9.3 \pm 2.2	7.0 \pm 1.4	5.2 \pm 1.0	4.1 \pm 0.8	7.4 \pm 2.3	
Cl ⁻	7.7 \pm 1.4	6.9 \pm 1.7	7.0 \pm 1.9	6.4 \pm 1.4	4.5 \pm 1.3	7.4 \pm 1.8	4.2 \pm 1.3	5.2 \pm 1.3	2.0 \pm 0.6	5.7 \pm 1.4	
	4.1 \pm 1.1	4.8 \pm 1.6	3.7 \pm 1.1	3.2 \pm 1.6	1.9 \pm 0.3	2.9 \pm 1.8	1.6 \pm 0.5	1.9 \pm 0.7	0.6 \pm 0.3	2.7 \pm 1.0	
NO ₃ ⁻	6.5 \pm 1.9	6.1 \pm 1.9	5.7 \pm 1.8	5.3 \pm 2.0	4.4 \pm 1.0	5.7 \pm 1.5	4.7 \pm 0.8	3.3 \pm 0.8	2.3 \pm 0.5	4.9 \pm 1.4	
	2.9 \pm 1.7	3.1 \pm 1.5	2.7 \pm 1.3	3.8 \pm 2.1	2.1 \pm 0.6	3.0 \pm 0.8	2.5 \pm 0.7	1.6 \pm 0.3	1.5 \pm 0.4	2.6 \pm 1.1	
SO ₄ ²⁻	24.8 \pm 4.4	22.2 \pm 5.6	21.0 \pm 4.3	19.3 \pm 4.4	14.9 \pm 3.4	23.8 \pm 6.1	14.8 \pm 4.5	17.1 \pm 3.7	7.4 \pm 1.3	18.5 \pm 4.2	
	14.2 \pm 5.1	15.5 \pm 5.1	13.1 \pm 1.9	10.8 \pm 4.7	6.9 \pm 1.8	11.4 \pm 3.5	7.5 \pm 2.8	9.3 \pm 2.6	3.9 \pm 0.8	10.3 \pm 3.2	

a) At the 0.01 significance level, the difference between dry and wet means is statistically significant (*t*-test) at all locations.

b) All values are $\mu\text{g m}^{-3} \pm$ SD. Each value is a mean of eight samples.

kilns located in the study area was also a likely source of trace metals such as Cd, Zn, Cu, and Pb [19, 24]. These metal concentrations are mostly due to anthropogenic emissions, so maxima were found at locations characterized by intensive industrial and vehicular activities nearby (e.g., http://uk-air.defra.gov.uk/assets/documents/reports/cat16/0604041205_heavy_metal_issue1_final.pdf) [21, 30].

Among the water-soluble cations and anions in PM, NH_4^+ , and SO_4^{2-} were found to have the highest concentration. The NO_3^- concentration in PM was found less as compared to the SO_4^{2-} concentration. Nitrate is almost invariably observed indicating excess ammonia in the atmosphere that neutralizes the particulate sulfate and condenses with the nitrate, forming particulate ammonium sulfate ($(\text{NH}_4)_2\text{SO}_4$) and ammonium nitrate (NH_4NO_3) [14]. These secondary ions concentration is associated with the long-distance sources and enhanced gas to particle conversion [19]. K^+ and Cl^- ions are mostly emitted by coal, biomass, and waste burning as well these ions are also associated with a crustal origin [4]. Spatial and temporal variations in TSP and its element concentrations were mainly due to changes in

anthropogenic activities and prevailing metrological conditions [1, 2, 9, 15, 24, 31], as will be explored further in what follows.

3.2 Source identification from elemental wind roses

To identify the possible sources in the study area, the wind roses for the selected elements at each sampling location were superimposed on the map of the study area. All pollutant wind roses are presented in Supporting Information Figs. S5–S14. The maps showing superimposed wind roses with vectors drawn toward the direction of the highest peak from each location for Cd, Ni, and Fe are presented in Figs. 2–4, respectively, and for other selected elements in Supporting Information Figs. S15–S21.

As a first order assessment, sources are identified as lying at a given distance along a straight line from the point of measurement in the direction of peak average concentration [10–12]. In this study Cd, Ni, and Fe are identified as tracers of specific sources, i.e., brick kilns, oil-fueled power plant/refinery, and traffic related

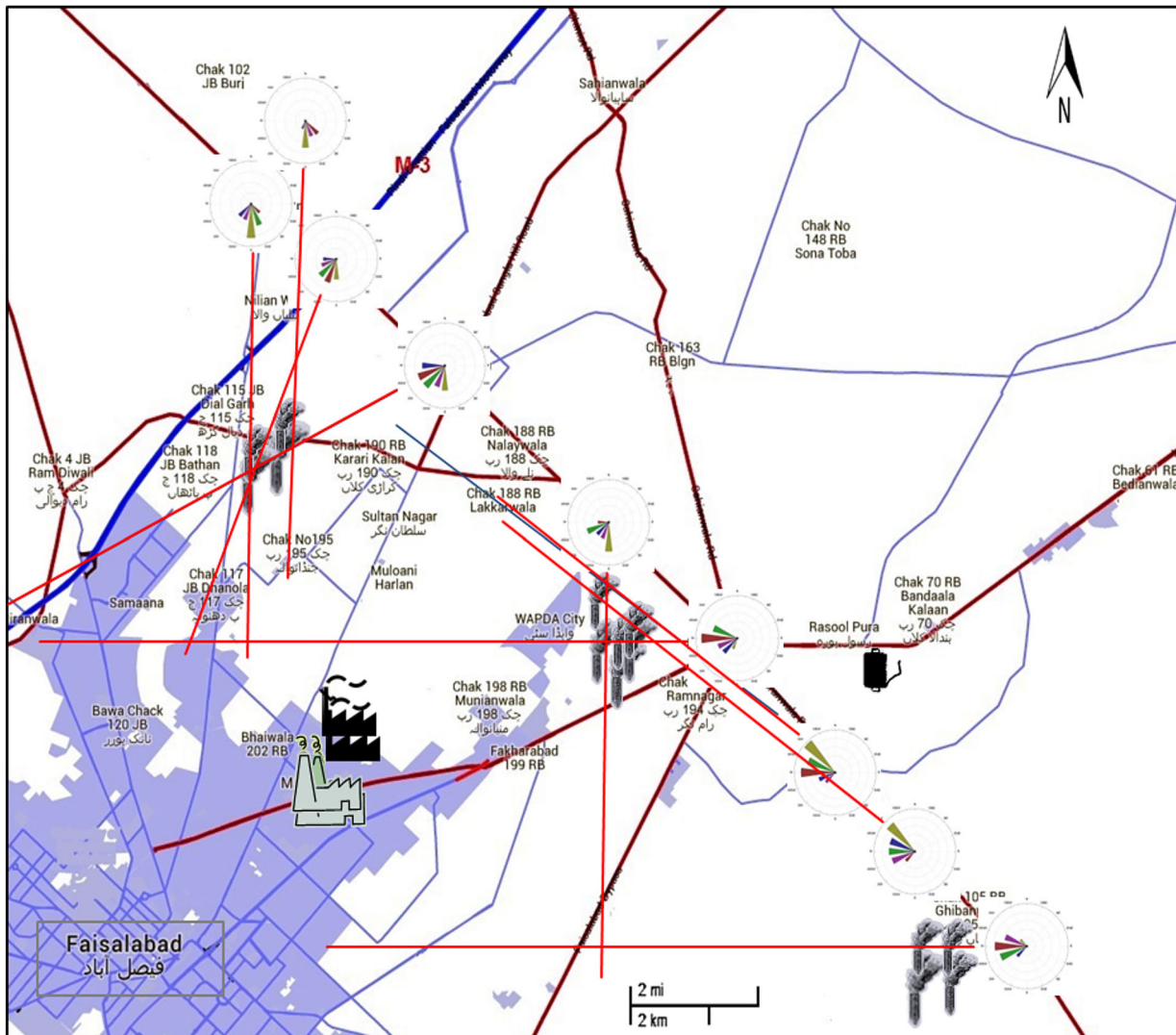


Figure 2. Map with superimposed Cd wind roses with the direction of concentration peaks pointing the direction of the potential source from the sampling location.

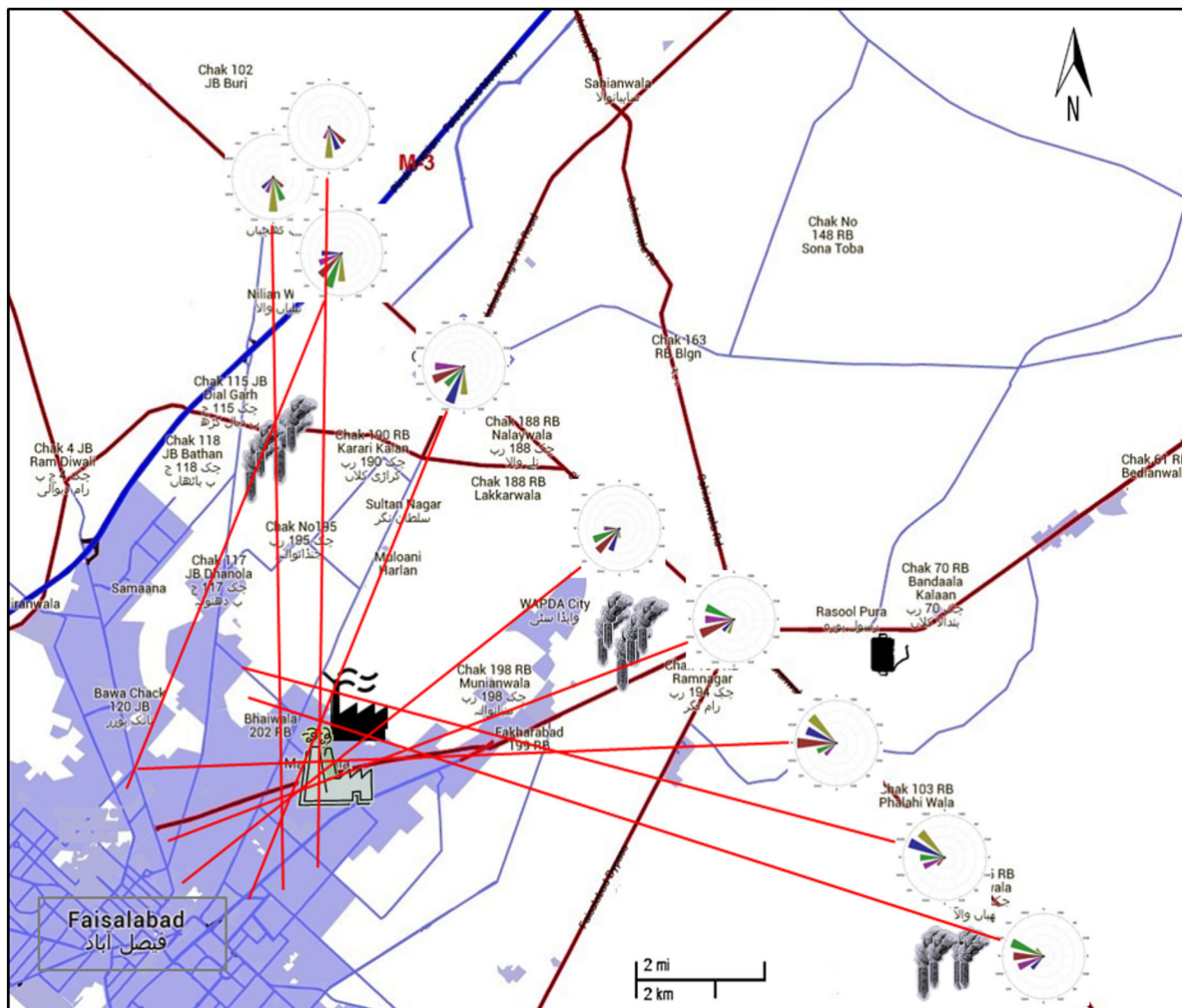


Figure 3. Map with superimposed Ni wind roses with the direction of concentration peaks pointing the direction of the potential source from the sampling location.

resuspended road dust, respectively, that are likely existing sources in the study area as indicated by Javed et al. [19]. The selected elements are tracers of these sources as frequently reported in the literature [2, 4–6, 13–15, 21, 24, 31, 32].

The Cd concentration wind rose peaks indicate the directions for Cd sources relative to the sampling locations. Hence, the intersection of vectors drawn from each sampling location triangulates likely sources. Figure 2 suggests that the likely sources of Cd are brick kilns located at the intersection of Cd vectors. More than 600 brick kilns operate in and around Faisalabad. Among these, seven are located in the study area upwind from the sampling locations (Fig. 1). Low-quality coal, wood, used rubber tires, and waste oil are mostly used for fuel in these kilns. This low-quality fuel, combined with inefficient combustion process produces vast quantities of hazardous air pollutants including trace metals such as Cd, Zn, Pb, Na, and K (see Supporting Information Figs. S15–S21 for the wind rose maps for the other elements associated with brick kilns) [4, 15, 19, 33, 34].

A power plant consisting of two units with a production capacity of 132 and 244 MW is also situated upwind from sampling locations. A PARCO oil refinery is about 500 m from the power

plant. Ni has been reported as a tracer of the petrochemical industry and oil combustion (power plant and oil refinery) [13, 31, 24]. The concentration peaks of Ni wind roses at all sampling locations are directed toward the power plant and oil refinery location (Fig. 3).

Traffic-related resuspended road dust is also a dominant source of aerosol PM and mainly contributed Fe, Mg, Ca, Cu, and Pb (see Fig. 4 and Supporting Information Figs. S15–S21 for maps for the other elements) to atmospheric PM metals. Iron was used as a typical tracer of resuspended soil/road dust emissions [1, 13–15, 24, 28]. The longest petals of the Fe wind roses point toward roadways, the largest sources of resuspended dust (Fig. 4). Roads in Faisalabad are poorly maintained, heavily trafficked, and have unpaved shoulders with limited, poor vegetation along the sides. Vehicle fleets are typically old, poorly maintained, employing inefficient engines, overloaded, smoky, and use fuel of poor quality [4, 29].

In summary, the convolution of element concentrations with wind direction indicates the direction of the main emissions and triangulation of these directions from multiple sites coincides with the location of known major sources in the study area.

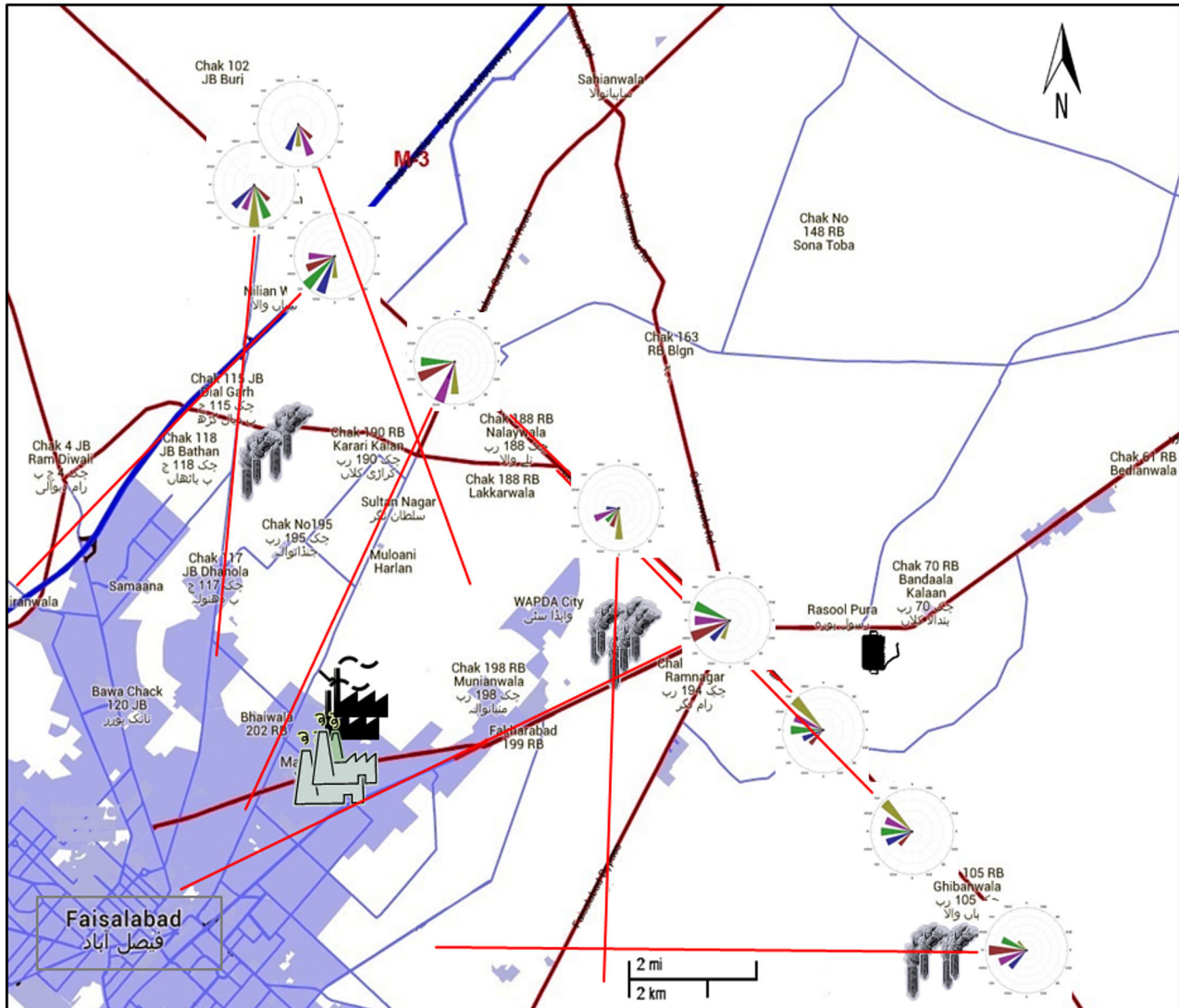


Figure 4. Map with superimposed Fe wind roses with the direction of concentration peaks pointing the direction of the potential source from the sampling location.

3.3 Source identification from directionally oriented UNMIX results

The UNMIX model was run separately on the elemental concentrations associated with the directions of the three possible sources identified by the wind rose analysis (e.g., power plant/refinery, brick kilns, and roadways). UNMIX results are shown in Fig. 5a–c, which represent the distribution of each element across the source profiles, derived from the model. The first component in each presumably corresponds to the signature of the source category indicated by the wind rose triangulations. For the power plant directional dataset ($n=68$), source 1 was interpreted as power plant/oil refinery as expected, because of high factor loadings on elements Ni, Zn, and Pb in this source, which could be due to the use of crude oil in power plant and oil refinery. These tracer elements are useful indicators of this emission source [13, 21, 24, 30]. Source 2 will be discussed below.

Source 1 for the brick kiln directional dataset ($n=64$) suggests its elemental profile. It is characterized by high loadings of the

elements Cd, Na, Zn, and Pb, possibly from the combustion of low-quality fuel currently being used in brick kilns located in the study area [4, 14, 15, 19, 34]. Again, source 2 will be discussed below.

The UNMIX results regarding roadway directional dataset ($n=78$) also resolved two sources. Source 1, likely from resuspended road dust, is typical of crustal elements, e.g., Fe, Mg, and Ca [1, 13, 15, 28]. Considerable levels of Zn, Pb, and Cu were also found in this source profile and attributed to the poor vehicle maintenance and the use of adulterated fuel [4, 35]. For instance, Pb is still being used as an anti-knock agent in gasoline despite a ban on leaded fuel because compliance is not enforced yet. So, Pb has become a part of the road dust due to the use of leaded fuel over the years [14, 19, 29]. Zn and Cu are emitted from lubricant oil, brake linings, and tire wear [31, 36].

This roadway source profile closely resembles source 2 of both power plant and brick kiln dataset suggesting strong resemblance with each other. The second source in the roadway dataset could be

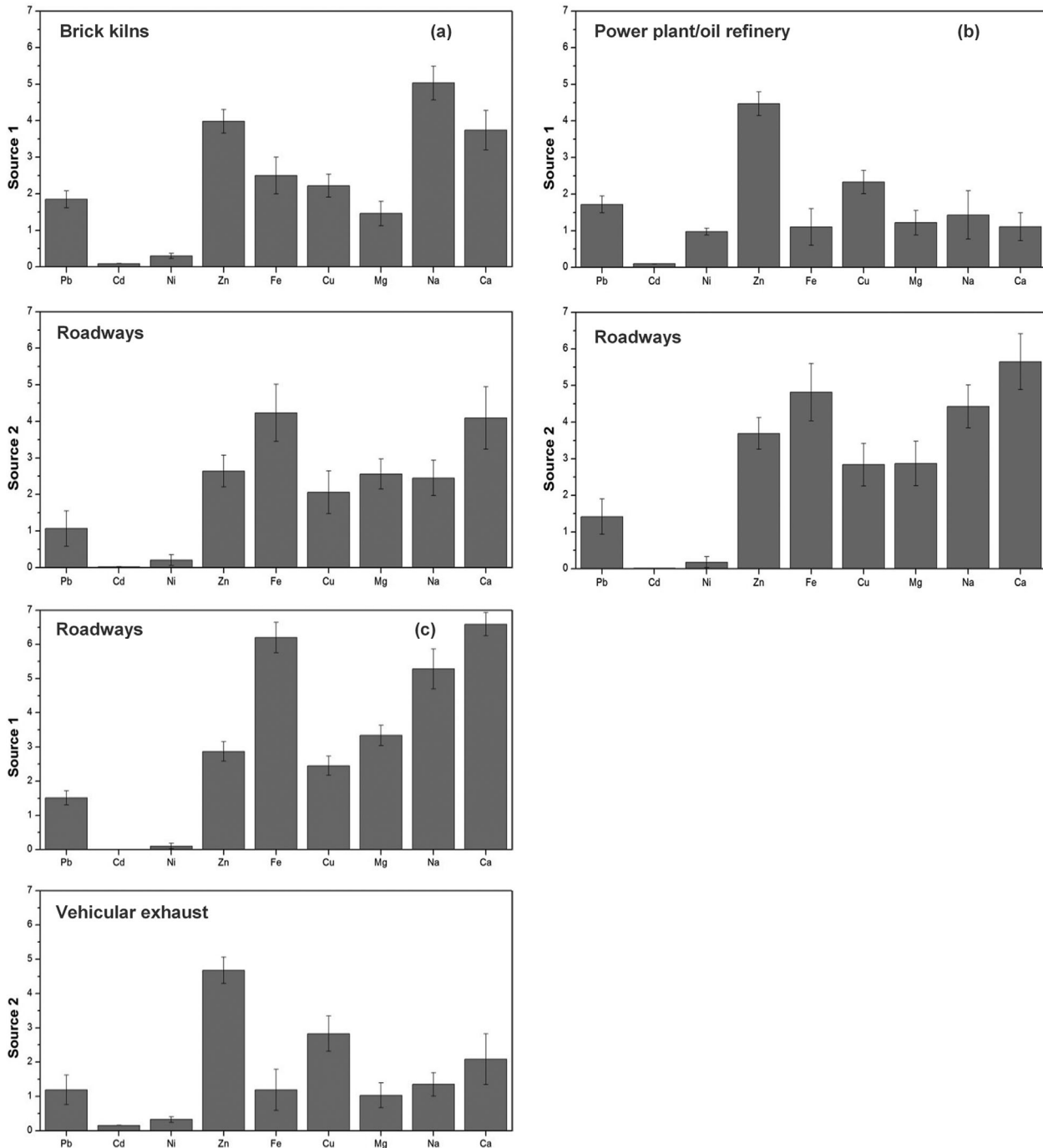


Figure 5. UNMIX-derived source contributions ($\mu\text{g m}^{-3}$) for the dataset of (a) brick kilns (b) power plant/oil refinery (c) roadways.

electric generators and vehicular exhaust due to high loading of Pb, Zn, and Cu [14, 31, 36].

In this study, the normalized dot product was successfully used to quantify the similarity between different source profiles extracted from UNMIX model runs on various datasets [22]. The normalized dot product between the roadway sources 1 and 2 for the power plant and brick kiln source are 0.99 and 0.98, respectively. Normalized dot products between all profiles are listed in Tab. 2 for comparison.

3.4 Source identification from overall UNMIX results

UNMIX was also run on the entire sample dataset for dry ($n = 216$) and wet ($n = 72$) seasons, separately. The three sources profiles obtained for the dry season (Fig. 6a) are similar to the first source profiles derived from the three directionally oriented UNMIX results. As shown in Tab. 2, the normalized dot products for the power plant, brick kiln, and roadway are 0.94, 0.98, and 0.99,

Table 2. Normalized dot products of the source profiles

Dataset	Sources	Dry season			Wet season		Roadway		Power plant		Brick kiln	
		S1	S2	S3	S1	S2	S1	S2	S1	S2	S1	S2
Dry season	S1	1.00	0.83	0.82	0.95^{a)}	0.77	0.78	0.90	0.94	0.84	0.87	0.83
	S2		1.00	0.92	0.81	0.90	0.92	0.87	0.86	0.76	0.98	0.92
	S3			1.00	0.87	0.97	0.99	0.78	0.73	0.98	0.90	0.99
Wet season	S1				1.00	0.82	0.83	0.84	0.95	0.90	0.93	0.87
	S2					1.00	0.99	0.71	0.65	0.98	0.91	0.97
Roadway	S1						1.00	0.73	0.67	0.99	0.92	0.98
	S2							1.00	0.91	0.82	0.86	0.80
Power plant	S1								1.00	0.77	0.84	0.75
	S2									1.00	0.94	0.98
Brick kiln	S1										1.00	0.90
	S2											1.00

^{a)}The largest (close to 1) values of dot product are marked in bold, showing the strong resemblance with each other.

respectively, confirming the three primary sources contributing to TSP during the dry season obtained from the directional analysis. The normalized dot products between the dry season source profile 3 (roadways) and directional analysis source profile 2 for the power

plant and brick kiln (roadways) are 0.98 and 0.99, respectively, again indicating roadways.

For the wet season, UNMIX resolved two sources (Fig. 6b) which can be interpreted as a power plant (source 1) and roadways (source

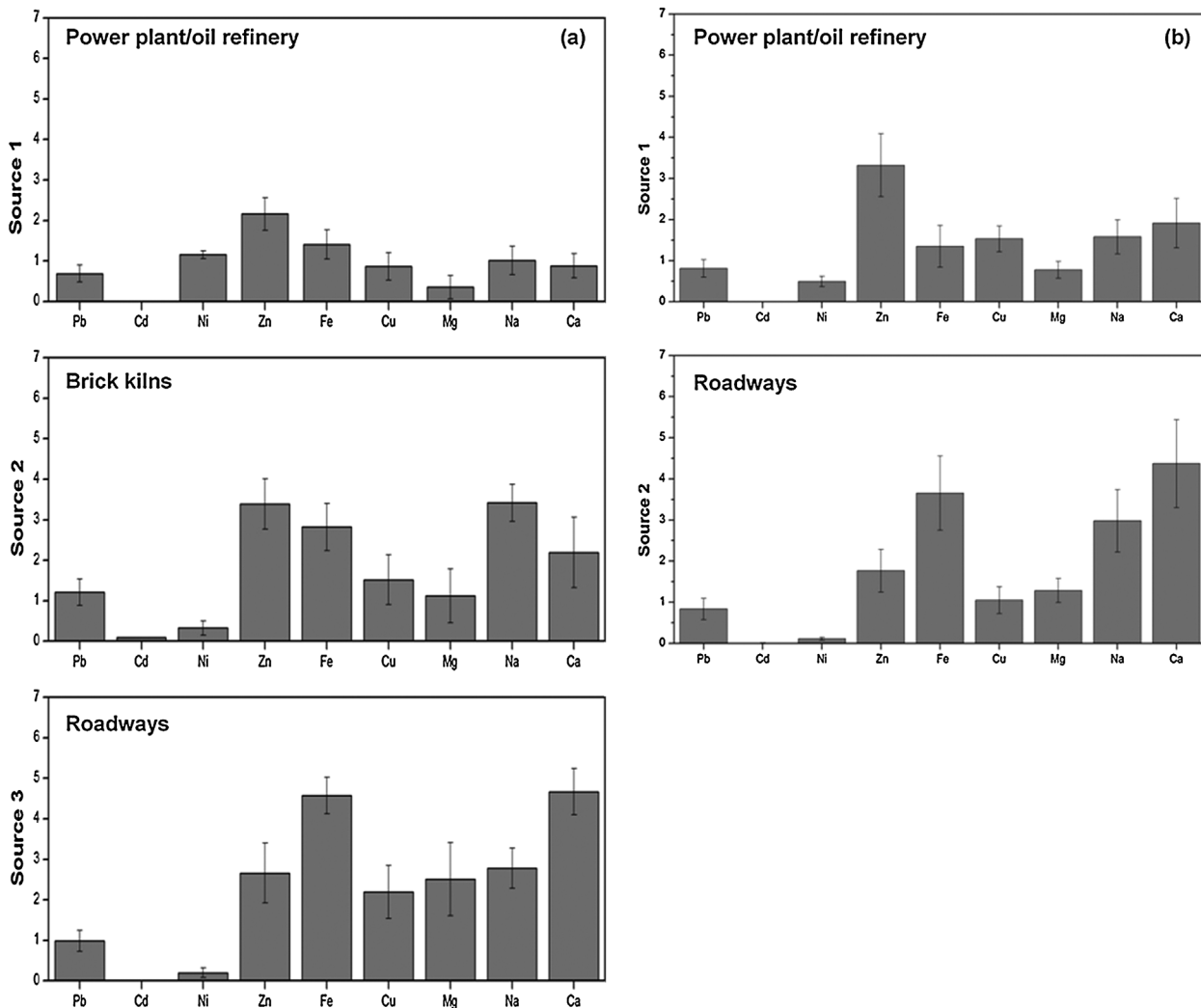


Figure 6. UNMIX resolved source profiles with element contributions ($\mu\text{g m}^{-3}$) (a) for the dry season (b) for the wet season.

Cu, and Zn) emerged as minor contributors. Source identification based on combined wind direction analysis and UNMIX results identified three major contributors to TSP: power plant/refinery, brick kilns, and roadways. The triangulation of the wind rose directions from multiple sites coincided with the location of known primary sources in the study area. The UNMIX results also identified elemental signatures corresponding to the same three primary sources indicated by the wind rose triangulations. The normalized dot product was successfully used to quantify the similarity between different source profiles extracted from UNMIX model runs on various datasets. The coupling of UNMIX with wind direction analysis proved thus to be useful in extracting more specific information on source contributions and locations. It is anticipated that the present investigation would be helpful for the designing and instituting the effective abatement strategies and emissions regulations.

Acknowledgments

The funding provided by Higher Education Commission, Government of Pakistan, to carry out this research is gratefully acknowledged. The study is a part of a Ph.D. research work of the corresponding author who would also like to thank personnel from the Air Quality Research Center, UC Davis for the writing assistance.

The authors have declared no conflicts of interest.

References

- [1] M. H. Shah, N. Shaheen, Annual and Seasonal Variations of Trace Metals in Atmospheric Suspended Particulate Matter in Islamabad, Pakistan, *Water Air Soil Pollut.* **2008**, *190*, 13–25.
- [2] M. H. Shah, N. Shaheen, Seasonal Behaviors in Elemental Composition of Atmospheric Aerosols Collected in Islamabad, Pakistan, *Atmos. Res.* **2010**, *95*, 210–223.
- [3] C. A. Pope III, Review: Epidemiological Basis for Particulate Air Pollution Health Standards, *Aerosol Sci. Technol.* **2000**, *32*, 4–14.
- [4] M. H. Shah, N. Shaheen, R. Nazir, Assessment of the Trace Elements Level in Urban Atmospheric Particulate Matter and Source Apportionment in Islamabad, Pakistan, *Atmos. Pollut. Res.* **2012**, *3*, 39–45.
- [5] R. Nazir, N. Shaheen, M. H. Shah, Indoor/Outdoor Relationship of Trace Metals in the Atmospheric Particulate Matter of an Industrial Area, *Atmos. Res.* **2011**, *101*(3), 765–772.
- [6] E. von Schneidmesser, E. A. Stone, T. A. Quraishi, M. M. Shafer, J. J. Schauer, Toxic Metals in the Atmosphere in Lahore, Pakistan, *Sci. Total Environ.* **2010**, *408*(7), 1640–1648.
- [7] M. A. Qadir, J. H. Zaidi, Characteristics of the Aerosol Particulates in the Atmosphere in an Urban Environment at Faisalabad, Pakistan, *J. Radioanal. Nucl. Chem.* **2006**, *267*, 545–550.
- [8] M. Ragosta, R. Caggiano, M. D'Emilio, M. Macchiato, Source Origin and Parameters Influencing Levels of Heavy Metals in TSP in an Industrial Background Area of Southern Italy, *Atmos. Environ.* **2002**, *36*, 3071–3087.
- [9] M. Zheng, L. G. Salmon, J. J. Schauer, L. Zeng, C. S. Kiang, Y. Zhang, G. R. Cass, Seasonal Trends in PM_{2.5} Source Contributions in Beijing, China, *Atmos. Environ.* **2005**, *39*, 3967–3976.
- [10] R. C. Henry, Y. S. Chang, C. H. Spiegelman, Locating Nearby Sources of Air Pollution by Nonparametric Regression of Atmospheric Concentrations on Wind Direction, *Atmos. Environ.* **2002**, *36*, 2237–2244.
- [11] M. Rigby, R. Timmis, R. Toumi, Similarities of Boundary Layer Ventilation and Particulate Matter Roses, *Atmos. Environ.* **2006**, *40*, 5112–5124.
- [12] G. Cosemans, J. Kretzschmar, C. Mensink, Pollutant Roses for Daily Averaged Ambient Air Pollutant Concentrations, *Atmos. Environ.* **2008**, *42*, 6982–6991.
- [13] Y. Song, S. D. Xie, Y. H. Zhang, L. Zeng, L. G. Salmon, M. Zheng, Source Apportionment of PM_{2.5} in Beijing Using Principal Component Analysis/Absolute Principal Component Scores and UNMIX, *Sci. Total Environ.* **2006**, *372*, 278–286.
- [14] A. Chakraborty, T. Gupta, Chemical Characterization and Source Apportionment of Submicron (PM₁) Aerosol in Kanpur Region, India, *Aerosol Air Qual. Res.* **2010**, *10*, 433–445.
- [15] T. Gupta, A. Mandariya, Sources of Submicron Aerosol During Fog-Dominated Wintertime at Kanpur, *Environ. Sci. Pollut. Res.* **2013**, *20*, 5615–5629.
- [16] US EPA, in *Compendium of Methods for the Determination of Inorganic Compounds in Ambient Air*, Method IO-3.1, US EPA, Cincinnati, OH, **1999**.
- [17] US EPA, in *Compendium of Methods for the Determination of Inorganic Compounds in Ambient Air*, Method IO-3.2, US EPA, Cincinnati, OH **1999**.
- [18] S. Jammalamadaka, U. Lund, The Effect of Wind Direction on Ozone Levels: A Case Study, *Environ. Ecol. Stat.* **2006**, *13*, 287–298.
- [19] W. Javed, G. Murtaza, H. R. Ahmad, S. M. A. Basra, A Preliminary Assessment of Chemical Constituents of Atmospheric Particulate Matter and Their Sources in Faisalabad, Pakistan, *J. Chem. Soc. Pak.* **2015**, *37*(4), 830–840.
- [20] US EPA, *EPA UNMIX 6.0, Fundamentals & User Guide*, Environmental Protection Agency, Office of Research and Development, Washington, DC **2007**.
- [21] Z. Mijic, A. Stojic, M. Perisic, S. Rajsic, M. Tasic, Receptor Modeling Studies for the Characterization of PM₁₀ Pollution Sources in Belgrade, *Chem. Ind. Chem. Eng. Q.* **2012**, *18*, 623–634.
- [22] X. H. Song, P. K. Hopke, Classification of Single Particles Analyzed by ATOFMS Using an Artificial Neural Network, ART-2A, *Anal. Chem.* **1999**, *71*, 860–865.
- [23] J. Tang, B. Jiang, B. Luo, in *Graph-Based Representations in Pattern Recognition* (Eds.: X. Jiang, M. Ferrer, A. Torsello), Springer, Berlin/Heidelberg **2011**, p. 175.
- [24] V. Celo, E. Dabek-Zlotorzynska, in *Urban Airborne Particulate Matter, Environmental Science and Engineering* (Eds.: F. Zereini, C. L. S. Wiseman), Springer, Heidelberg **2010**, p. 19.
- [25] WHO, *Air Quality Guidelines*, 2nd ed., WHO Regional Office for Europe, Copenhagen **2000**.
- [26] US EPA, *Revised Air Quality Standards for Particle Pollution and Updates to the Air Quality Index (AQI)*, Environmental Protection Agency, Office of Air Quality Planning and Standards, Research Triangle Park, NC **2012**.
- [27] Z. B. Yuan, A. K. H. Lau, H. Y. Zhang, J. Z. Yu, P. K. K. Louie, J. C. H. Fung, Identification and Spatiotemporal Variations of Dominant PM₁₀ Sources Over Hong Kong, *Atmos. Environ.* **2006**, *40*, 1803–1815.
- [28] J. Gu, M. Pitz, J. Schenlle-Kreis, J. Diemer, A. Reller, R. Zimmermann, J. Soentgen, et al., Source Apportionment of Ambient Particles: Comparison of Positive Matrix Factorization Analysis Applied to Particle Size Distribution and Chemical Composition Data, *Atmos. Environ.* **2011**, *45*, 1849–1857.
- [29] I. Colbeck, Z. A. Nasir, S. Ahmad, Z. Ali, The State of Ambient Air Quality in Pakistan – A Review, *Environ. Sci. Pollut. Res.* **2010**, *17*, 49–63.
- [30] K. Vincent, N. Passant, *Assessment of Heavy Metal Concentrations in the United Kingdom*, AEAT/ENV/R/2013/Issue 1, AEA Technology, London **2006**.
- [31] Z. Mijic, A. Stojic, M. Perisic, S. Rajsic, M. Tasic, M. Radenkovic, J. Joksic, Seasonal Variability and Source Apportionment of Metals in the Atmospheric Deposition in Belgrade, *Atmos. Environ.* **2010**, *44*, 3630–3637.
- [32] P. Pant, R. M. Harrison, Critical Review of Receptor Modeling for Particulate Matter: A Case Study of India, *Atmos. Environ.* **2012**, *49*, 1–12.
- [33] M. J. Kleeman, G. R. Cass, Source Contributions to the Size and Composition Distribution of Urban Particulate Air Pollution, *Atmos. Environ.* **1998**, *32*, 2803–2816.
- [34] V. Shridhar, P. S. Khillare, T. Agarwal, S. Ray, Metallic Species in Ambient Particulate Matter at Rural and Urban Location of Delhi, *J. Hazard. Mater.* **2010**, *175*, 600–607.

- [35] J. N. Gangwar, T. Gupta, A. K. Agarwal, Composition and Comparative Toxicity of Particulate Matter Emitted From a Diesel and Biodiesel Fuelled CRDI Engine, *Atmos. Environ.* **2012**, *46*, 472–481.
- [36] M. J. Kleeman, S. G. Riddle, M. A. Robert, C. A. Jakober, Lubricating Oil and Fuel Contributions to Particulate Matter Emissions From Light-Duty Gasoline and Heavy-Duty Vehicles, *Environ. Sci. Technol.* **2008**, *42*, 235–242.
- [37] A. K. Gupta, K. Karar, A. Srivastava, Chemical Mass Balance Source Apportionment of PM10 and TSP in Residential and Industrial Sites of an Urban Region of Kolkata, India, *J. Hazard. Mater.* **2007**, *142*, 279–287.
- [38] N. C. Kavuri, K. K. Paul, N. Roy, TSP Aerosol Source Apportionment in the Urban Region of the Indian Steel City, Rourkela, *Particuology* **2015**, *20*, 124–133.
- [39] A. Srivastava, S. Gupta, V. K. Jain, Winter-time Size Distribution and Source Apportionment of Total Suspended Particulate Matter and Associated Metals in Delhi, *Atmos. Res.* **2009**, *92*(1), 88–99.
- [40] R. M. Tripathi, A. V. Kumar, S. T. Manikandan, S. Bhalke, T. N. Mahadevan, V. D. Puranik, Vertical Distribution of Atmospheric Trace Metals and Their Sources at Mumbai, India, *Atmos. Environ.* **2004**, *38*, 135–146.
- [41] A. Salam, H. Bauer, K. Kassim, S. M. Ullah, H. Puxbaum, Aerosol Chemical Characteristics of a Mega-City in Southeast Asia (Dhaka-Bangladesh), *Atmos. Environ.* **2003**, *37*, 2517–2528.
- [42] M. N. Mondol, M. Khaled, A. S. Chamon, S. M. Ullah, Trace Metal Concentration in Atmospheric Aerosols in some City Areas of Bangladesh, *Bangladesh J. Sci. Ind. Res.* **2015**, *49*(4), 263–270.